THE ASTROPHYSICAL JOURNAL, 509:L17–L20, 1998 December 10

ATOMIC CARBON IN ARP 220

MARYVONNE GERIN[1,2] AND THOMAS G. PHILLIPS[3]

Received 1998 August 3; accepted 1998 October 15; published 1998 October 26

ABSTRACT

We present detections of the $^3P_1$–$^3P_0$ fine-structure line of neutral carbon and of the $J = 3$–2 rotational line of carbon monoxide in the ultraluminous infrared galaxy Arp 220, obtained at the Caltech Submillimeter Observatory. C I emission in Arp 220 is found to be at the expected level in relation to the strong far-infrared (FIR) dust emission and to the CO emission, whereas the C II emission seen by the *Infrared Space Observatory* long-wavelength spectrometer is very weak. The C I data confirm the presence of a large mass of molecular gas in the nucleus of Arp 220, corresponding to a high extinction in the visible ($A_v = 1000$). For this galaxy, the total cooling due to atomic carbon is comparable to the total cooling due to carbon monoxide. We use the observed C I/CO (1–0) and CO (3–2)/CO (1–0) emissivity ratios, together with the photon-dominated region models, to infer an average gas density of $n(H_2) \approx 10^4$ cm^{-3}. We estimate the UV radiation field in this galaxy from the FIR continuum, and independently from hydrogen recombination lines, to be about a factor of 40,000 larger than in the solar vicinity ($G_0 = 4 \times 10^4$). The relative weakness of the C II fine-structure line is explained by the large gas density, the exceptionally strong UV field, and the large dust opacity. C II emission from high-redshift analogs of Arp 220 may not be as easy to detect as had been anticipated. However, both CO and C I lines will still be strong emitters.

Subject headings: galaxies: individual (Arp 220) — galaxies: interactions — galaxies: ISM — galaxies: starburst — ISM: atoms — radio lines: galaxies

1. INTRODUCTION

The ultraluminous infrared galaxy (ULIRG) Arp 220 (=UGC 9913 = IC 4553) is one of the closest examples ($V_{\rm hel} = 4550$ km s^{-1}, $D = 77$ Mpc) of the end product of galaxy interactions. The central region looks like an elliptical galaxy with an $r^{1/4}$ luminosity profile and two very close nuclei, while the outer regions still have a disturbed morphology. The spectral energy distribution is dominated by the very strong far-infrared (FIR) emission from dust. There is strong, widely dispersed CO emission (Casoli et al. 1988; Radford et al. 1991) but, surprisingly, relatively weak C II (158 μm) emission (Fischer et al. 1997). The C I emission observations presented here provide extra information to assist in resolving the physical situation.

The origin of the energy source for the FIR radiation has long been debated. Is it due mostly to an active nucleus, a burst of star formation, or both? Recent data point to star formation as the most likely energy source (Genzel et al. 1998; Smith et al. 1998a, 1998b). High-resolution images of the stellar distribution (with the *Hubble Space Telescope* Near-Infrared Camera and Multiobject Spectrometer; Scoville et al. 1998) and of the gas (Scoville, Yun, & Bryant 1997) show that the star-forming activity and dense molecular gas are concentrated in a molecular disk of 250 pc radius (=0$''$.67), which accounts for $\frac{2}{3}$ of the CO emission. A more extended envelope (up to 1.5 kpc radius = 4$''$) contributes the other $\frac{1}{3}$ of the CO flux. The radiation from massive stars that are formed in the dense disk is very efficiently trapped by dust grains and reprocessed into FIR wavelengths, leading to a huge extinction ($A_v \sim 1000$) for the mixture of gas and stars. The shape of the FIR spectral energy distribution is well fitted by a modified blackbody, with a dust temperature of ∼50 K, and a dust opacity reaching at least 1 at 150–200 μm (Scoville et al. 1991; Fischer et al. 1997). In the submillimeter, the dust emissivity scales as $\lambda^{-\beta}$ with $\beta = 1.3$ (Scoville et al. 1991) to 1.75 (Fischer et al. 1997). The FIR spectrum (43–197 μm) obtained with the long-wavelength spectrometer (LWS) of the *Infrared Space Observatory* (*ISO*) is dominated by dust emission, with some absorption lines of water vapor and OH and with the fine-structure line of ionized carbon at 158 μm as a sole, weak, emission line (Fischer et al. 1997; Luhman et al. 1997, 1998). At shorter wavelengths, fine-structure lines of ionized neon, sulfur, and silicon and recombination lines of hydrogen have been detected in emission with the *ISO* short-wavelength spectrometer (Genzel et al. 1998; Sturm et al. 1996). At longer wavelengths, where dust is optically thin, the CO and C I (this work) lines are seen in emission. Table 1 summarizes the information on Arp 220. The C II line is only $\sim 1.3 \times 10^{-4}$ of the total FIR flux, whereas it is generally in the range of 10^{-2}–10^{-3} (Stacey, Geis, & Genzel 1991; Malhotra et al. 1997).

In fact, it has been noted that weak C II emission is a common property of ULIRGs with heavily obscured stellar radiation ($L_{\rm FIR}/L_B \geq 10$) (Luhman et al. 1998; Malhotra et al. 1997). For starburst galaxies, the intense CO and C II emission is mainly produced in numerous photon-dominated regions (PDRs) at the surface of molecular clouds (Stacey et al. 1991). The weak C II emission in Arp 220 is presumably caused either by unusual physical conditions in the galaxy PDRs, leading to low C II production, or by optical depth effects in both the dust and the C II line (Luhman et al. 1997).

Atomic carbon is another important diagnostic of PDRs, since the models predict that the recombination of C$^+$ with electrons leads to the formation of a neutral carbon layer at an intermediate depth inside the cloud (A_v of a few magnitudes). At greater depths, the carbon should be fully locked into the stable molecule CO. In fact, this view has been somewhat modified because of the observations of molecular clouds

[1] Radioastronomie millimétrique–URA, 336 du CNRS, Laboratoire de Physique de l'ENS, 24 Rue Lhomond, F-75231 Paris Cedex 5, France; maryvonne.gerin@physique.ens.fr.

[2] DEMIRM-URA, 336 du CNRS, Observatoire de Paris, 61 Avenue de l'Observatoire, F-75014 Paris, France.

[3] Caltech Submillimeter Observatory, 111 Nowelo Street, Hilo, HI 96720; phillips@tacos.caltech.edu.

TABLE 1
EMISSION CHARACTERISTICS OF ARP 220

Line	W (K km s^{-1})	Flux (W m^{-2})	Luminosity ($L_\odot$)	HPBW (arcsec)	Reference
CO (1–0)	109	1.8×10^{-18}	3.3×10^5	22	1
CO (2–1)	155	7.9×10^{-18}	1.5×10^6	13	1
^{13}CO (1–0)	≤5	$\leq 8.3 \times 10^{-20}$	1.5×10^4	22	2
^{13}CO (2–1)	8.5	4.3×10^{-19}	7.9×10^5	13	2
CO (3–2)	32 ± 3.5	1.7×10^{-17}	3.1×10^6	20	3
C I ($^3P_1$–$^3P_0$)	23 ± 3.8	1.9×10^{-17}	3.5×10^6	15	3
C II ($^2P_{3/2}$–$^2P_{1/2}$)		8.7×10^{-16}	1.6×10^9	80	4
FIR		6.8×10^{-12}	1.2×10^{12}		
CO-tot		2.1×10^{-16}	3.9×10^7		
C I–tot		1.0×10^{-16}	1.8×10^7		

REFERENCES.—(1) Radford et al. 1991; (2) Casoli, Dupraz, & Combes 1992; (3) this work; (4) Fischer et al. 1997.

NOTE.—The adopted distance is 77 Mpc.

showing that neutral carbon is found with a much more extended distribution than the predictions of homogeneous chemical models (see, e.g., Keene et al. 1996). In any case, atomic carbon is found to be a good tracer of molecular gas and plays a strong role in the total cooling of the gas. In the case of Arp 220, it also provides further information that can help to resolve the problem of the weak C II line. In this Letter, we report the detection in Arp 220 of the $^3P_1$–$^3P_0$ fine-structure line of atomic carbon and of the $J = 3$–2 rotational line of carbon monoxide, using the Caltech Submillimeter Observatory (CSO).

2. OBSERVATIONS

The C I and CO (3–2) observations were performed at the CSO, in 1998 March, using SIS receivers operated in double-sideband mode. In good atmospheric conditions ($\tau_{225\,\mathrm{GHz}} \leq 0.06$), the system temperature usually ranges between 1000 and 3000 K. The observations were performed using a chopping secondary mirror, with the throw set to 1′ on the sky. The spectra were analyzed with an acousto-optic spectrometer with a total bandwidth of 1500 MHz (of which only 900 MHz is used, because of the bandwidth limit of the receivers) and a resolution of about 2 MHz. The main-beam efficiencies of the CSO were 0.65 and 0.53 at 345 and 492 GHz, respectively; the corresponding conversion factors between janskys and kelvins (T_A^*) are 70 and 100 Jy K^{-1}.

For Arp 220, the C I line is redshifted to 483.374 GHz; the receiver was tuned with the signal in the upper sideband in order to avoid contamination by the telluric line of molecular oxygen at 487 GHz. Because Arp 220 has very broad lines (~500 km s^{-1} = 800 MHz at 483 GHz), we used three different receiver settings to obtain a complete coverage of the line, with central velocities at −300, 0, and 300 km s^{-1} relative to the line center. First, we used the spectra taken at velocity offsets 300 and −300 km s^{-1} to adjust the zero level of the baseline, with a window set from −370 to 370 km s^{-1} by reference to the published CO spectra (Radford et al. 1991). We then computed the baseline offset for the central spectrum, to minimize the platforming effects with the spectra taken at 300 and −300 km s^{-1}. The overlap region is quite large, 70–200 km s^{-1} on the right side for example. The offset was in fact zero, and no platforming was evident. Both the CO (3–2) and C I lines have similar shapes to those of the CO lines observed at the IRAM 30 m telescope (Radford et al. 1991). The CSO spectra are shown in Figure 1.

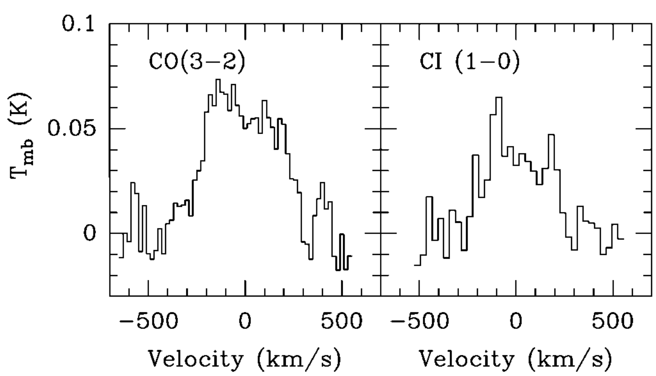

FIG. 1.—$J = 3$–2 line of carbon monoxide (*left*) and a $^3P_1$–$^3P_0$ line of atomic carbon (*right*) in Arp 220 observed with the CSO. The temperature scale is $T_{\rm mb}$ in kelvins. The position has been taken from Condon et al. (1991) and is R.A. (1950) = 15$^{\rm h}$32$^{\rm m}$46$^{\rm s}$.9, decl. (1950) = 23°40′08″. The central velocity is $V_{\rm LSR}$ = 5450 km s^{-1} (cz).

3. RESULTS

3.1. *Column Density of Molecular Hydrogen*

Table 1 reports the measured fluxes for the emission of the FIR continuum, C II, C I, and three CO lines. The average column density of molecular gas in the telescope beam can be deduced from the strength of the C I line. The measured signal in Arp 220 corresponds to a column density of atomic carbon of $N(\mathrm{C}) = 1.25 \times 10^{16} \int T\,dv = 2.8 \times 10^{17}$ cm^{-2} in the 15″ CSO beam. Frerking et al. (1989) have shown that the carbon abundance relative to H_2 has a maximum value of 2.2×10^{-5} for $A_v = 4$–11 mag and does not deviate from this value by more than a factor of 4 for larger A_v's. The column density of molecular hydrogen is thus at least 1.2×10^{22} cm^{-2} in the CSO beam. This corresponds to a mass of molecular gas of at least $6.2 \times 10^9\ M_\odot$, including helium. The value for the column density of molecular hydrogen deduced from C I can be compared directly with the estimate deduced from CO (1–0). Using the conversion factor deduced from *COS B* data (Strong et al. 1988), we obtain a column density of 2.5×10^{22} cm^{-2} in the 22″ beam of the IRAM 30 m telescope. The CO method, therefore, probably overestimates slightly the column density of molecular hydrogen for this case. A similar conclusion was reached by Scoville et al. (1997).

Scoville et al. (1997) mapped the CO emission at high angular resolution in Arp 220 and showed that $\frac{2}{3}$ of the CO emission comes from a thin disk of 0″.67 radius (250 pc for their assumed distance of 77 Mpc) and that $\frac{1}{3}$ comes from a more extended envelope. Assuming that these numbers also hold for C I, we can correct the C I emission for the beam filling factor of the dense disk and directly obtain the column density of molecular material in this disk. The beam filling factor of a 1$''$.33 diameter source is 8×10^{-3}; hence, a lower limit to the column density of molecular hydrogen is $\frac{2}{3} \times 1.2 \times 10^{22}/8 \times 10^{-3} = 10^{24}$ cm^{-2}. Assuming a disk thickness of 16 pc, the average gas density in the disk is $n(H_2) \sim 2 \times 10^4$ cm^{-3}.

The large column density corresponds to a huge extinction in the visible for the "mixture" of dust, gas, and stars: $A_v = 1000$ mag, in agreement with Scoville et al. (1997) and Genzel et al. (1998). This generates significant opacity in the dust in the FIR. Using the dust emissivity parameters deduced from the analysis of the *COBE* data (Boulanger et al. 1996), $\tau(\lambda)/N_{\rm H} = 10^{-25}(\lambda/250\ \mu m)^{-2}$ cm^2, the dust opacity at 158 μm (the C II wavelength) is at least 0.5. In fact, the dust emissivity is known to increase by a factor of ∼2 in dense molecular gas, compared with diffuse gas (Mezger, Wink, & Zylka 1990; Goldsmith, Bergin, & Lis 1997), so the dust opacity at 158 μm is about 1 for the material in the dense disk. The total is even larger since the diffuse material associated with the extended CO emission will contribute also.

3.2. *Gas Cooling*

To estimate the total cooling due to atomic carbon and CO, it is necessary to estimate the power radiated in other lines, which is not observed so far: C I (2–1) at 809 GHz and CO (4–3), . . ., (7–6). C I (2–1) has been detected in M82 (Stutzki et al. 1997) with the same brightness temperature as C I (1–0). For M82, a nearby starburst galaxy, the cooling due to C I (2–1) is a factor of 4.4 larger than that due to the 492 GHz line alone. Data for CO lines in M82 are reported by Güsten et al. (1993). Assuming similar C I line ratios for Arp 220 and M82, and also similar CO line ratios, we obtain the total cooling due to C and CO as listed in Table 1. If we use instead the Galactic center as a template (Bennett et al. 1994), we find roughly 40% of the power estimated using M82 as a template. The total cooling due to CO and C therefore represents about 4.6×10^{-5} of the total luminosity of Arp 220, and 35% of the cooling due to C^+.

For dense cool gas, as seen toward the Galactic center, the main contributions to the CO cooling comes from the $J =$ 3–2, 4–3, and 5–4 lines (Bennett et al. 1994). Detection of CO (6–5) in Arp 220 would indicate the presence of warmer and denser material than is seen toward the Galactic center, where this line is barely detected by *COBE*/FIRAS. Güsten et al. (1993) report CO (4–3) and (6–5) data for some external galaxies. In a starburst galaxy like M82, CO (6–5) and other higher J CO lines contribute most of the cooling due to CO lines, whereas CO (6–5) is weak in a normal spiral galaxy like NGC 6946. Observations of high-J CO lines with submillimeter telescopes will be extremely useful for getting a better measurement of the thermal budget. Although it is weaker relative to the dust emission in Arp 220 than in nearly all galaxies, C II ($^2P_{3/2}$–$^2P_{1/2}$) is still the main cooling line of the gas.

3.3. *Physical Conditions*

The combination of the measurements of the C II, CO (1–0), and FIR continuum fluxes is often used to get constraints on the radiation and gas density, using PDR models (Stacey et al. 1991). From the large FIR flux and apparent low C II flux for Arp 220, Fischer et al. (1997) deduced quite unusual physical conditions, with very dense gas ($n \sim 10^5$ cm^{-3}) and a low UV field, $G_0 = 20$ relative to the UV field in the solar neighborhood [I(6–13.6 eV) $= 1.4 \times 10^{-4}$ ergs s^{-1} cm^{-2} sr^{-1}; Mathis, Mezger, & Panagia 1983]. The use of PDR models relies on the hypothesis that the FIR, CO, and C II emission are produced in the same region, and are diluted by the same factor in the beam, since the models have been developed for a single molecular cloud (Wolfire, Hollenbach, & Tielens 1989; Stacey et al. 1991). For Arp 220 and other ULIRGs, the relative geometry of stars and gas is different from that in starburst galaxies, as indicated by the much larger extinction in the visible. Contrary to the situation in spiral and starburst galaxies, where a significant fraction of the UV light produced by massive stars escapes the galaxy [τ(2000 Å) ∼ 0.9; Buat & Burgarella 1998], in Arp 220 virtually all radiation from massive stars is converted to FIR dust emission (Genzel et al. 1998). Whereas star formation occurs in a small region, as indicated by the distribution of bright supernova remnants (0$''$.2 × 0$''$.4 toward the northwest nucleus; Smith et al. 1998b), the absorption of UV radiation and the conversion to FIR radiation may occur over a more extended region, including both the dense molecular disk and the diffuse envelope (Scoville et al. 1997). This extended envelope can be considered as a PDR with a low UV illumination, hence producing little C II emission per unit hydrogen atom. In fact, a lower limit to the size of the FIR emission can be set assuming that the galaxy emits as a blackbody at $T = 50$ K. We find a source diameter of 1$''$.6 at 100 μm. This matches the size of the dense molecular disk. Also, Arp 220 appears to be slightly extended at 10 μm (Miles et al. 1996).

Generally, PDR models predict C^+ (and, for dense gas, O) fine-structure lines to be the main cooling lines of the gas for most of the parameter space, with a moderate opacity for the C II line [τ(C II) ∼ 1; Wolfire et al. 1989] and larger opacities for the oxygen lines. For most galaxies, the dust opacity in the FIR is low, and the medium is transparent for the line emission. For Arp 220, the individual PDRs, both in the dense disk and in the diffuse envelope, add up to produce so much dust emission that it becomes optically thick in the FIR. This affects the C II line but not the CO and C I lines that appear at longer wavelengths, where the dust opacity is still small. The same dust in molecular clouds close to H II regions is responsible for the large extinction suffered by the hydrogen recombination lines (Genzel et al. 1998). Because the massive stars and H II regions are distributed in the same volume as the molecular gas and dust, the radiative transfer is described by the "mixed" formula, which, for Arp 220, indicates a total extinction of $A_v \sim 1000$ mag. It is possible that the C II line itself may also develop a large optical depth (Luhman et al. 1998), but this will depend on the precise geometry and velocity structure of the galaxy, so we do not attempt to deal with that effect here.

The fact that the continuum opacity is nonnegligible at 158 μm in Arp 220 hampers the direct use of PDR models to explain the C II data. Since significant dust opacity is observed in Arp 220, the observed C II flux should be corrected for this effect. With a dust opacity of at least 1, the correction factor to the C II flux is at least $\tau/[1 - \exp(-\tau)] \sim 1.6$, for dust mixed with the C II sources.

To obtain information on the star-forming regions, other lines at longer wavelengths must be used, such as the fine-structure lines of atomic carbon and the rotational lines of carbon monoxide. Here we have available the C I (1–0) and CO (3–2) lines. In PDR models, the emissivity ratios, C I (1–0)/CO (1–0) and CO (3–2)/CO (1–0), vary with the gas density (Le Bourlot et al. 1993; Bakes & Tielens 1998). The observed Arp 220 ratios are consistent with moderately dense gas, $n \sim 10^4$ cm^{-3}.

It is more difficult to set constraints on the UV flux from the observed lines, because neither CO nor C I (1–0) lines are very sensitive to G_0. However, the observed recombination lines and free-free continuum radiation from Arp 220 correspond to a Lyman continuum photon production rate of $N_{\rm Lyc} = 6 \times 10^{54}$ s^{-1}, and $L_{\rm Lyc} \sim 4 \times 10^{10}\ L_{\odot}$ (Genzel et al. 1998) with large uncertainties. We choose the above value deduced from radio recombination lines since it is free from extinction (Zhao et al. 1996). Using this value for $L_{\rm Lyc}$, the average radiation field in a 1″.33 diameter disk is 6.8 ergs cm^{-2} s^{-1} sr^{-1} for the ionizing radiation. The field in the UV (6–13.6 eV) is at least as intense as the ionizing radiation for a typical population of massive stars; thus, the average field in the UV is $G_0 = 6.8/1.4 \times 10^{-4} = 4.8 \times 10^4$ relative to the interstellar radiation field in the solar neighborhood. We can obtain an independent estimate for the UV field from the FIR radiation since we know that all the stellar radiation is down-converted to the FIR. We use as a reference for the radiation field the bolometric radiation in the solar neighborhood, $I(0.912\text{–}1000\ \mu m) = 2.1 \times 10^{-3}$ ergs cm^{-2} s^{-1} sr^{-1} (Mathis et al. 1983), and a source diameter of 1″.6 for $\frac{2}{3}$ of the FIR luminosity, since this is the blackbody diameter for the Arp 220 FIR source. The FIR-derived enhancement factor is then $G_{\rm FIR} = 4.4 \times 10^4$. Thus, we obtain typical PDR conditions for the dense molecular gas in Arp 220 of $n \geq 10^4$ cm^{-3}, $G_0 \approx 4 \times 10^4$. The predicted $C^+/F_{\rm UV}$ ratio in these conditions is $\leq 5 \times 10^{-4}$, with an excitation temperature of ∼100 K. As we have seen, the predicted C II flux has to be corrected to take into account the attenuation of the line by the dust opacity implied by the large FIR continuum, giving $\leq 3 \times 10^{-4}$. The observed C II/FIR is about 1.3×10^{-4}.

4. CONCLUSION

This Letter reports the detection of C I (1–0) and CO (3–2) in Arp 220. By comparing these lines with the known CO (1–0) emission, we obtained the following estimates of the physical conditions in Arp 220: the average gas density is high, 10^4 cm^{-3}, and the UV radiation field deduced from the radio recombination lines and the FIR flux is 4×10^4 more intense than the UV radiation field in the solar neighborhood. We have estimated the total cooling due to C and CO in Arp 220 to be 4.6×10^{-5} of the total luminosity of Arp 220, and 35% of the cooling due to C^+. The total cooling effects due to C and CO are similar, with $L(\text{C-tot}) = 1.8 \times 10^7\ L_{\odot}$ and $L(\text{CO-tot}) = 3.9 \times 10^7\ L_{\odot}$.

For a merger galaxy with a small and dense starburst region and a more extended envelope of diffuse gas, the intensity of the FIR fine-structure lines coming from the PDRs in the starburst zone is suppressed relative to the dust emission, by the high value of the UV field and also by the dust opacity in the envelope, resulting in surprisingly weak C II emission. Submillimeter lines of CO and C I are therefore better diagnostics of the starburst. From the measured C I and CO lines, and with the help of a PDR code, we are able to predict a C II/FIR ratio $\leq 3 \times 10^{-4}$, which is reasonably close to the *ISO*-LWS measured value of $\approx 10^{-4}$.

We thank J. Le Bourlot, G. Pineau des Forêts, and E. Roueff for the use of their PDR model and J. Fischer for providing *ISO*-LWS spectra. The CSO is funded by NSF contract AST96-15025. M. Gerin acknowledges travel grants from INSU/CNRS and NATO.

REFERENCES

Bakes, E. L. O., & Tielens, A. G. G. M. 1998, ApJ, 499, 258
Bennett, C. L., et al. 1994, ApJ, 434, 587
Boulanger, F., et al. 1996, A&A, 312, 256
Buat, V., & Burgarella, D. 1998, A&A, 334, 772
Casoli, F., et al. 1988, A&A, 192, L17
Casoli, F., Dupraz, C., & Combes, F. 1992, A&A, 264, 55
Condon, J. J., Huang, Z. P., Yin, Q. F., & Thuan, T. X. 1991, ApJ, 378, 65
Fischer, J., et al. 1997, in Proc. First *ISO* Workshop on Analytical Spectroscopy, ed. A. M. Heras (SP-419; Noordwijk: ESA), 149
Frerking, M. A., Keene, J., Blake, G. A., & Phillips, T. G. 1989, ApJ, 344, 311
Genzel, R., et al. 1998, ApJ, 498, 579
Goldsmith, P. F., Bergin, E. A., & Lis, D. C. 1997, ApJ, 491, 615
Güsten, R., Serabyn, E., Kasemann, C., Schinkel, A., Schneider, G., Schultz, K., & Young, K. 1993, ApJ, 402, 537
Keene, J., Lis, D. C., Phillips, T. G., & Schilke, P. 1996, in IAU Symp. 178, Molecules in Astrophysics: Probes and Processes, ed. D. J. Jansen, M. R. Hogerheijde, & E. F. van Dishoeck (Leiden: Sterrewacht), 129
Le Bourlot, J., Pineau des Forêts, G., Roueff, E., & Flower, D. 1993, A&A, 267, 233
Luhman, M. L., Satyapal, S., Fischer, J., & Wolfire, M. G. 1997, in Proc. First *ISO* Workshop on Analytical Spectroscopy, ed. A. M. Heras (SP-419; Noordwijk: ESA), 283
Luhman, M. L., et al. 1998, ApJ, 504, L11
Malhotra, S., et al. 1997, ApJ, 491, L27
Mathis, J. S., Mezger, P. G., & Panagia, N. 1983, A&A, 128, 212
Mezger, P. G., Wink, J. E., & Zylka, R. 1990, A&A, 228, 95
Miles, J. W., Houck, J. R., Hayward, T. L., & Ashby, M. L. N. 1996, ApJ, 465, 191
Radford, S., et al. 1991, ApJ, 368, L15
Scoville, N. Z., et al. 1998, ApJ, 492, L107
Scoville, N. Z., Sargent, A. I., Sanders, D. B., & Soifer, B. T. 1991, ApJ, 366, L5
Scoville, N. Z., Yun, M. S., & Bryant, P. M. 1997, ApJ, 484, 702
Smith, D. A., et al. 1998a, ApJ, 494, 150
Smith, H. E., Lonsdale, C. J., Lonsdale, C. J., & Diamond, P. J. 1998b, ApJ, 493, L17
Stacey, G. J., Geis, N., & Genzel, R. 1991, ApJ, 373, 423
Strong, A. W., et al. 1988, A&A, 207, 1
Sturm, E., et al. 1996, A&A, 315, L133
Stutzki, J., et al. 1997, ApJ, 477, L33
Wolfire, M. G., Hollenbach, D., & Tielens, A. G. G. M. 1989, ApJ, 344, 770
Zhao, J. H., Anantharamaiah, K. R., Goss, W. M., & Viallefond, F. 1996, ApJ, 472, 54